Engineering integrin signaling for promoting embryonic stem cell self-renewal in a precisely defined niche

Seung Tae Lee [a], Jung Im Yun [a], Yun Suk Jo [a], Mayumi Mochizuki [a], André J. van der Vlies [a], Stephan Kontos [a], Jong Eun Ihm [a], Jeong M. Lim [c], Jeffrey A. Hubbell [a,b,*]

[a] Institute of Bioengineering, Ecole Polytechnique Fédérale de Lausanne, CH-1015 Lausanne, Switzerland
[b] Institute of Chemical Sciences and Engineering, Ecole Polytechnique Fédérale de Lausanne, CH-1015 Lausanne, Switzerland
[c] Major in Biomodulation, WCU, Department of Agricultural Biotechnology, Seoul National University, 151-921 Seoul, Republic of Korea

ARTICLE INFO

ABSTRACT

We present development and use of a 3D synthetic extracellular matrix (ECM) analog with integrin-specific adhesion ligands to characterize the microenvironmental influences in embryonic stem cell (ESC) self-renewal. Transcriptional analysis of 24 integrin subunits followed by confirmation at the translational and functional levels suggested that integrins $\alpha_5\beta_1$, $\alpha_v\beta_5$, $\alpha_6\beta_1$ and $\alpha_9\beta_1$ play important roles in maintenance of stemness in undifferentiated mouse ESCs. Using the well-defined matrix as a tool to activate integrins $\alpha_5\beta_1$ plus $\alpha_v\beta_5$, $\alpha_6\beta_1$ and $\alpha_9\beta_1$, individually and in combination, differential integrin activation was demonstrated to exert exquisite control over ESC fate decisions. Simultaneous ligation of these four integrin heterodimers promoted self-renewal, as evidence by prolonged SSEA-1, Oct4 and Nanog expression, and induced Akt1 kinase signaling along with translational regulation of other stemness-related genes. The biofunctional network we have designed based on this knowledge may be useful as a defined niche for regulating ESC pluripotency through selective cell–matrix interactions, and the method we present may be more generally useful for probing matrix interactions in stem cell self-renewal and differentiation.

1. Introduction

The nature of the niche that enables prolonged self-renewal of ESCs remains only partially elucidated. An often used, but poorly understood, such environment is provided by mouse embryonic fibroblasts (MEFs), which present substantial difficulties in systematic investigations because of their presentation of myriad signals to the ESCs. Several attempts have been described to replace MEF feeder layers with ECM proteins and matrices such as Matrigel, ECM derived from MEFs, etc. [1–3]. These biologically derived materials are also very complex and are not subject to control at the molecular level. Synthetic hydrogel and fibrillar matrices have been explored, in an attempt to replace such complicated biological materials with defined artificial materials for short-term ESC culture [4,5], yet these materials still do not present the fullness of the ECMs repertoire of molecular characteristics. Sophisticated photochemical degradation approaches have been developed to explore the dynamic nature of cell-material interactions in the niche in artificial systems, for example the factors controlling stem cell chondrogenic differentiation [6].

ECM components can induce a variety of signals for functional regulation of cells, and the integrin family of cell surface adhesion receptors consisting of α and β subunits [7] regulates numerous such interactions related to biological process that include cell attachment, spreading, proliferation, survival, morphogenesis and gene expression [8–11], as well as critical steps of differentiation in early embryogenesis [7,12–16]. However, despite considering ECM signaling as an important factor in ESC self-renewal fate decisions [17,18], the literature remains unclear about the function of integrins in maintenance of the ESC self-renewal, except for self-renewal of adult stem cell [19–21], in part due to a lack of well characterized research tools. We have developed a synthetic ECM analog based on branched poly(ethylene glycol) (PEG) crosslinked with matrix metalloproteinase (MMP)-sensitive peptides and functionalized with peptide adhesion ligand [22,23]. Cells are able to interact with the matrix via the coupled adhesion peptides and to remodel the matrix via the MMPs they activate and present at the cell surface. Here, we functionalize these materials with multiple integrin-activating ligands with good control over the amounts and identities of the adhesion ligands for the purpose of elucidating the

* Corresponding author. EPFL, SV/IBI/LMRP, Station 15, CH-1015 Lausanne, Switzerland. Tel.: +41 21 693 9682; fax: +41 21 693 9665.
E-mail address: jeffrey.hubbell@epfl.ch (J.A. Hubbell).

influence exerted by the ECM on ESCs in their self-renewal fate decisions. These methods may more generally provide a defined niche for investigation of matrix interactions in stem cell self-renewal and differentiation.

2. Materials and methods

2.1. ESC culture

The mouse ESCs E14tg2a (CRL-1821, ATCC, Manassas, VA) were routinely cultured on a feeder layer of MEFs treated with 10 μg/ml mitomycin C (Sigma–Aldrich, St. Louis, MO) in 5% CO_2 at 37 °C in Dulbecco's modified Eagle's medium (DMEM; Gibco Invitrogen, Grand Island, NY) supplemented with 15% (v/v) heat-inactivated fetal bovine serum (FBS; HyClone, Logan, UT), 0.1 mM β-mercaptoethanol (Gibco Invitrogen), 1% (v/v) nonessential amino acids (NEAA; Gibco Invitrogen), 1 mM sodium pyruvate (Sigma–Aldrich), 2 mM L-glutamine (Gibco Invitrogen), a 1% (v/v) lyophilized mixture of penicillin and streptomycin (Gibco Invitrogen) and 1000 units/ml mouse leukemia inhibitory factor (LIF) (Chemicon International, Temecula, CA) (herein referred to as ESC culture medium). Subpassage was performed every third day and the medium was changed daily during subculture.

2.2. Quantitative real-time PCR

All the specific primer sequences shown in Supplementary Table 1 were designed with cDNA sequences obtained from GenBank for mouse and by Primer3 software (Whitehead Institute/MIT Center for Genome Research). Extraction of total mRNA from each group was conducted by using a RNeasy Plus Mini Kit (Qiagen, Valencia, CA) and cDNA was synthesized from ~1 μg of total mRNA using a Reverse Transcription System (Promega, Madison, WI). Gene expression was estimated by real-time quantitative PCR using iQ™ SYBR® Green Supermix (Bio-Rad Laboratories, Hercules, CA). The PCR amplification was performed on the Bio-Rad iCycler iQ system (Bio-Rad Laboratories) in a final volume of 25 μl using cycling parameters (3 min, 95 °C; 30 s, 95 °C; 30 s, 60 °C; 30 s 72 °C, with the latter three steps repeated for 40 times). The melting curve data were collected to check the PCR specificity. By identifying the absence of dimerization between primers through control real-time PCR reaction lacking template, 300 nM in the all primers was selected as the final optimized concentration. The mRNA level of each sample for each gene was normalized to that of β-actin mRNA. Relative mRNA level was presented as $2^{-\Delta\Delta Ct}$, where Ct = threshold cycle for target amplification, $\Delta Ct = Ct_{target\ gene}$ (specific genes for each sample) $- Ct_{internal\ reference}$ (β-actin for each sample), and $\Delta\Delta Ct = \Delta Ct_{sample}$ (treatment sample in each experiment) $- \Delta Ct_{calibrator}$ (control sample in each experiment).

2.3. Western blot

Cell lysates were prepared by treatment of M-PER® Mammalian Protein Extraction Reagent (Pierce, Woburn, MA) supplemented with protease inhibitor cocktail (Roche Diagnostics, Indianapolis, IN) with protein concentration determination with a NanoDrop™ 1000 spectrophotometer (Thermo Fisher Scientific, Rockford, IL). Subsequently, the cell lysates (160 or 240 μg) were fractionated by 7.5, 10 or 15% (v/v) SDS-polyacrylamide gel, according to the molecular size of the protein of interest, and transferred onto a polyvinylidene difluoride membrane (Millipore, Billerica, MA). After blocking with 5% (w/v) skimmed milk (Bio-Rad laboratories) overnight at 4 °C, the membrane was washed three times with PBST consisting of PBS (pH 7.4; Gibco Invitrogen) and 0.1% Tween-20 (Sigma–Aldrich), and incubated with the primary antibodies listed in the Supplementary Table 2. After washing three times with PBST, the primary antibodies were detected by the appropriate horseradish peroxidase (HRP)-conjugated secondary antibodies listed in the Supplementary Table 2 and developed with enhanced chemiluminescent substrate (Pierce). Protein bands on membranes were visualized with CL-XPosur-e™Film (Thermo Fisher Scientific) and the intensities of individual protein bands were quantified by densitometry using a Bio-Rad Imaging System Quantity One ver. 4.5.1 with ChemiDoc XRS (Bio-Rad Laboratories).

2.4. Formation of PEG-based hydrogel, insertion of ESCs into PEG-hydrogel and culture

The PEG-based hydrogel was formed by the conjugation of vinylsulfone (Sigma–Aldrich)-functionalized 3arm-PEG (PEG-VS) synthesized as described [24] and dicysteine-containing peptides with an intervening matrix metalloproteinase (MMP)-specific cleavage site (Ac-GCRD-GPQGIWGQ-DRCG-NH₂) (herein referred to as crosslinker) through a Michael-type addition reaction [25]. For making a typical 10% (w/v) PEG-hydrogel into which ESC were incorporated, all the precursor solutions of PEG-VS (dissolved in ESC culture medium), crosslinker (dissolved in pH 8.0 0.3 M HEPES buffer) and ESCs (suspended in ESC culture medium) were mixed. For incorporation of ESCs into the PEG-hydrogel with specific integrin-binding adhesion peptides, firstly, the PEG-VS precursor solution was reacted with the precursor solution containing the adhesion peptides (in pH 8.0 0.3 M HEPES buffer) for 30 min at room temperature and this solution was then mixed with the precursor solutions of crosslinker and ESCs. Subsequently, gelation of a circular disk derived from 6 μl of the mixed precursor solutions occurred within 30 min at 37 °C [24] and the ESCs encapsulated into PEG-hydrogel were cultured in a humidified atmosphere of 5% CO_2 in air at 37 °C in the ESC culture medium and the medium was exchanged every day.

2.5. Peptide synthesis and purification

Peptides synthesis on solid resin (Novasyn TGR, Novabiochem, Laeuflfingen, Switzerland) was performed using an automated peptide synthesizer (Chemspeed, Augst, Switzerland) with standard Fmoc/HBTU/HOBT chemistry [24,25]. Purification of synthesized peptides was conducted by reverse phase chromatography on a C18 column (Biocad 700E; PerSpective Biosystems). The sequence of purified peptides were confirmed by matrix-assisted laser desorption ionization/time-of-flight (MALDI-TOF) mass spectrometry. The details of all the peptides utilized are shown in the Supplementary Table 3.

2.6. Flow cytometric analysis

The ESC population fixed in 4% (v/v) paraformaldehyde (Sigma–Aldrich) was washed in ice cold PBS and 1×10^6 ESC from the ESC population were distributed separately for analysis of stage specific embryonic antigen (SSEA)-1, Oct4 and Nanog expression. For staining SSEA-1, cell surface protein, the distributed ESCs were incubated for 1 h at 4 °C with primary anti-SSEA-1 (as shown in Supplementary Table 2) diluted in 2% (v/v) FBS-containing PBS, and this primary antibody was detected by incubating fluorescently conjugated secondary antibody (as shown in Supplementary Table 2) for 1 h at 4 °C. For staining Oct4 and Nanog, which exist in the nucleus as a transcription factor, ESCs were incubated for 1 h at 4 °C with fluorescently conjugated anti-Oct4 and anti-Nanog (as shown in Supplementary Table 2) diluted in Hanks' Balanced Salt Solution (HBSS; Gibco Invitrogen) supplemented with 0.1% (w/v) saponin (AppliChem Gmbh, Darmstadt, Germany) and 0.05% (w/v) sodium azide (Sigma–Aldrich). Subsequently, after washing sufficiently, the stained cells resuspended in 500 μl PBS were analyzed using flow cytometry, on a CyAn™ ADP Analyzer (Beckman Coulter, Inc., Fullerton, CA), and FLOWJO Ver. 7.2.5 software program (Tree Star, Inc., Ashland, OR).

2.7. ELISA

Preparation of cell lysates was conducted by using methods recommended from each ELISA manufacturer and the amount of cell lysates were quantified with a NanoDrop™ 1000 spectrophotometer. Subsequently, analysis by ELISA of total Stat3 (Gibco Invitrogen), phospho-Tyr705-Stat3 (Gibco Invitrogen), total β-catenin (Cell Signaling, Beverly, MA), total Akt1 (Cell Signaling), and phospho-Ser 473-Akt1 (Cell Signaling) protein assays were performed according to manufacturer's instructions.

2.8. Statistical analysis

All the numerical data derived from each experiment were analyzed statistically by the Statistical Analysis System (SAS) program. Moreover, when a significance of the main effects was detected by analysis of variance (ANOVA) in the SAS package, the least-square or DUNCAN methods were conducted to compare among treatments. Significant differences among treatments were determined where the p value was less than 0.05.

3. Results

3.1. Identification of integrin heterodimers expressed in undifferentiated embryonic stem cells (ESCs)

To provide guidance regarding which integrins may be present in the undifferentiated state, we monitored expression of integrin heterodimers in undifferentiated mouse ESCs. Transcriptional levels of genes encoding total 24 integrin subunits (Fig. 1a,d) were quantified, and integrin α_5, α_6, α_8, α_9 and α_v and integrin β_1, β_3, β_4, β_5 and β_7 showed higher expression levels than other subunits. By contrast, integrin α_1, α_3, α_4, α_7, α_{10}, α_{11}, α_L and α_N were minimally transcribed, while no expression of integrin α_2, α_D and α_X and integrin β_2, β_6 and β_8 were observed. When translation of the integrin α subunits showing increased transcription (α_5, α_6, α_9 and α_v) was evaluated, integrin α_5 subunit showed the highest translation in the amount of glycosylated mature and non-glycosylated immature proteins (Fig. 1b,f,h). The total amounts of integrin α_6 and
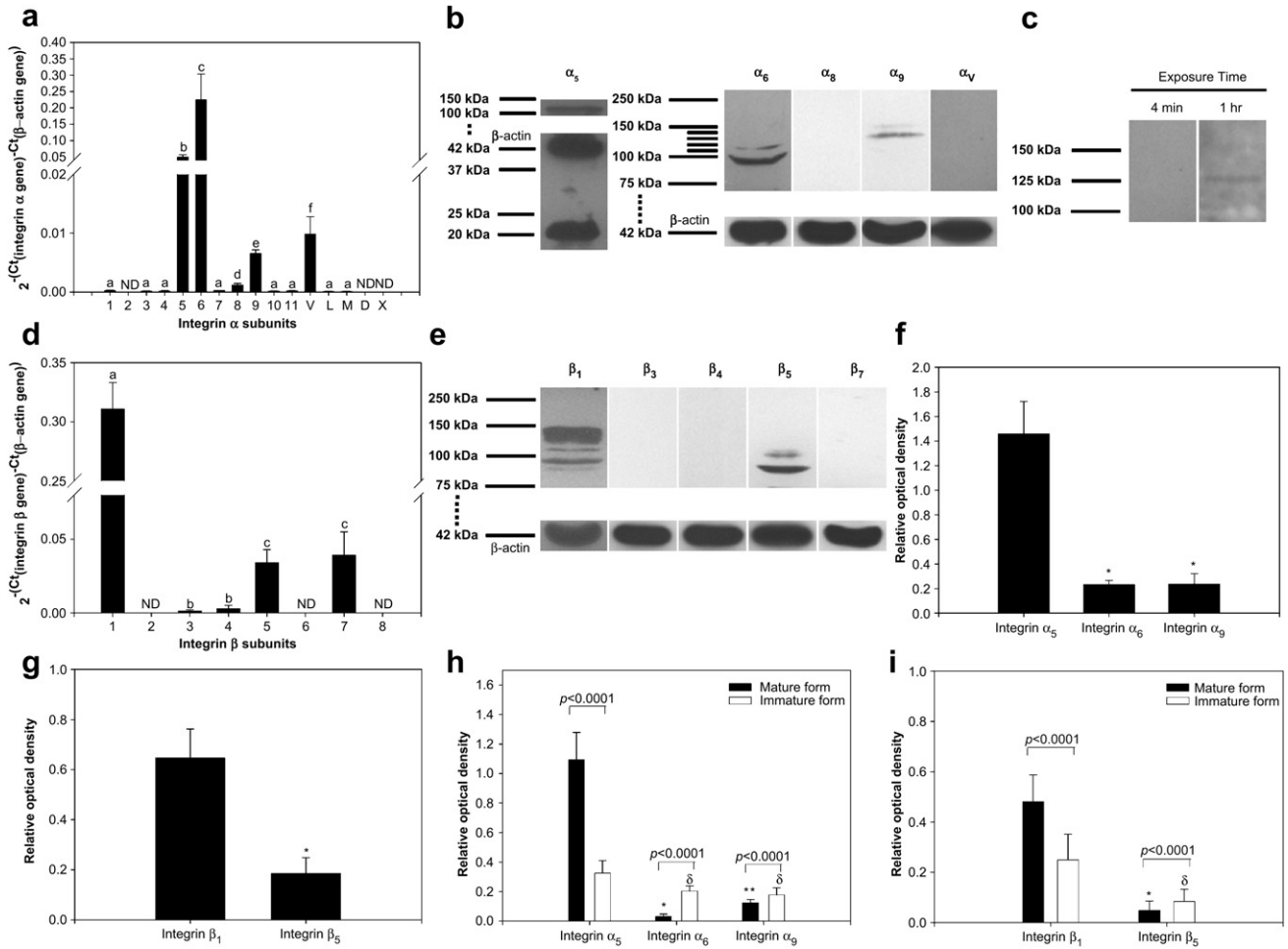
Fig. 1. Expression of integrin subunits in ESCs. (a) and (d) Transcriptional levels of the integrin α (a) and β (d) subunit genes in the ESCs. Among total 16 integrin α and 8 integrin β subunit genes, real-time PCR showed that transcriptional levels of 5 integrin α and 5 integrin β subunit genes were increased significantly. (b), (c) and (e) Western blot analysis of the integrin α (b and c) and β (e) subunit proteins expressed in the ESCs. The translational levels of integrin α_5, α_6, α_9, β_1, and β_5 subunits were identified by immunoblotting and exposing to the film for 4 min before densitometric analysis. Subsequently, a prolonged exposure up to 1 hr was performed for some integrin subunits (α_8, β_3, β_4, β_7 and α_v) showing no expression under standard protocol, but no expression was detected except for the case of integrin α_v (c). Both glycosylated mature and non-glycosylated immature forms were observed in integrin α_5, α_6, α_9, β_1 and β_5 subunits and densitometric analysis on each subunit was subsequently performed (f–i). Total amount of each integrin subunit protein expressed (f and g) and the translational levels of mature (with glycosylation) and immature (without glycosylation) protein in each subunit (h and i) are presented as the optical density relative to the level of β-actin protein expression on the same blot. The highest expressions in total amount of glycosylated mature and non-glycosylated immature proteins were found in integrin α_5 and β_1 subunit, respectively, and total amount of mature integrin α_5 and β_1 subunit proteins were expressed significantly more than that of immature proteins. In contrast, integrin α_6, α_9 and β_5 subunits showed significant decreases in the expression of mature protein relative to that of immature protein. All data shown are means ± S.D. of five independent experiments. $^{a,b,c,d,e,f}p < 0.05$, *, **$p < 0.05$, and $^{\delta}p < 0.05$. ND = not detected.

α_9 subunits were equal, but more translation of glycosylated mature protein was detected in integrin α_9 than integrin α_6 subunit (Fig. 1f,h). Integrin α_v subunit showed the lowest level among all up-regulated subunits (Fig. 1c). In the case of the integrin β subunits, only translation of β_1 and β_5 subunits was detected (Fig. 1e) and, regardless of glycosylation, the β_1 subunit showed more translation than the β_5 subunit (Fig. 1g,i). Integrin heterodimers $\alpha_5\beta_1$ and $\alpha_6\beta_1$ have been identified in ESCs to date [26,27]. Blocking integrin subunits α_5, α_6 and α_v or heterodimer $\alpha_9\beta_1$ in ESCs resulted in lowered adhesion to fibronectin, laminin, vitronectin and tenascin-C ECM components compared with non-blocking (Supplementary Fig. 1).

3.2. Optimization of the mechanical properties of a 3D scaffold for self-renewal of ESCs

We sought to utilize a hydrogel system developed by our laboratory as a 3D synthetic ECM analog [23,28], here using ligation of the above-discovered integrin heterodimers for supporting self-renewal of ESCs. A hydrogel network is formed *in situ*, in the presence of suspended cells, by crosslinking a reactive PEG vinyl-sulfone (PEG-VS) under near-physiological conditions with a di-cystyl peptide, the cysteine residues flanking a matrix metalloproteinase substrate site; adhesion ligands, formed as synthetic peptides with a free cysteine residue near the N-terminus, are linked within the network by the same reaction (Supplementary Fig. 2a). The mechanics of the hydrogel scaffold can be modulated by adjusting the stoichiometric ratio (r) of VS to cysteine equivalents. Neither a difference in mechanical elastic modulus (obtained by varying r from 0.6 to 1.1), nor difference in culture dimension (3D PEG-hydrogel scaffold vs. 2D coculture with or without a MEF feeder) was observed to influence the metabolic activity of ESCs (Supplementary Fig. 2c,e). Spherical ESC colonies formed uniformly 5 d after culture within PEG-hydrogels of any r level (Supplementary Fig. 2b upper panels), and the colonies were homogenously derived from the stem cells (Supplementary Fig. 2b lower panels). A

significant increase in the size of ESC colonies was detected in PEG-hydrogel of r from 0.6 or 1.1, i.e. the soft materials at the extrema of the range we explored. Whereas, despite PEG-hydrogel with 1.0 r was softer than those with 0.6 r, the significantly smaller size of colonies was observed (Supplementary Fig. 2d). This suggests that mechanical property of PEG-hydrogel is not the only factor that influences the proliferation of ESCs. Significant decreases in alkaline phosphatase (AP) activity and transcription of stemness-related genes were detected in the ESCs cultured in the absence of a MEF feeder layer. However, such decreases disappeared by the use of the 3D scaffold of different properties (Supplementary Fig. 2f,g); no prominent dependence in AP activity upon r was observed. The ESCs cultured within 3D scaffolds showed higher transcription of all stemness-related genes than the ESCs cultured in the feeder-free 2D system and, except for *Foxd3*, lower transcription than the ESCs cultured in the feeder-containing 2D system. Among the scaffolds of different r, the PEG-hydrogel of $r = 0.7$ fully supported ESC maintenance and was selected for further exploration.

3.3. Determination of adhesion peptide sequence binding specificity

We explored the effect of integrin heterodimer ligation upon self-renewal of undifferentiated ESCs. Based on the characterization described above, we selected integrins $\alpha_5\beta_1$, $\alpha_v\beta_5$, $\alpha_6\beta_1$ and $\alpha_9\beta_1$ for investigation (Fig. 1), using integrin-specific peptides for $\alpha_5\beta_1$ plus $\alpha_v\beta_5$, $\alpha_6\beta_1$, and $\alpha_9\beta_1$. The sequence RGDSP, derived from fibronectin, was used to primarily recognize integrin $\alpha_5\beta_1$ [29,30] and $\alpha_v\beta_5$; in this context, the soluble peptide prominently inhibited

binding of ESCs to fibronectin (Supplementary Fig. 3a) as well as to vitronectin [31] (Supplementary Fig. 3b). Conversely, suppressed attachment of ESCs to RGDSP peptide incorporated within the PEG hydrogels was detected after co-treatment of anti-integrin α_5 and anti-integrin α_v antibodies, more so than in response to either blocking antibody alone (Supplementary Fig. 3c). The angiogenesis inducer CCN1 [32]-derived sequence TTSWSQ was utilized for specificity to integrin $\alpha_6\beta_1$ activation. The transcriptional level of stemness-related genes in ESCs was prominently increased by the addition of soluble TTSWSQ peptide inside PEG-hydrogel, while anti-integrin α_6 antibody treatment significantly decreased the transcriptional levels even after being exposed to TTSWSQ peptide (Supplementary Fig. 4). The tenascin-C-derived sequence AEIDGIEL [33] was used for specificity versus integrin $\alpha_9\beta_1$; this peptide when soluble significantly inhibited attachment to tenascin-C (Supplementary Fig. 3d) and treatment with anti-integrin $\alpha_9\beta_1$ antibody remarkably blocked the binding of ESCs to AEIDGIEL peptide (Supplementary Fig. 3e). From these results, we confirmed the specificity of peptides containing RGDSP, TTSWSQ and AEIDGIEL for integrin $\alpha_5\beta_1$ as well as $\alpha_v\beta_5$, integrin $\alpha_6\beta_1$, and integrin $\alpha_9\beta_1$, respectively.

3.4. Effects of signaling through individual integrin ligation on ESC pluripotency

Having confirmed integrin specificity, we examined whether conjugation of the PEG-hydrogel with the adhesion peptides RGDSP, TTSWSQ or AEIDGIEL individually could support ESC self-
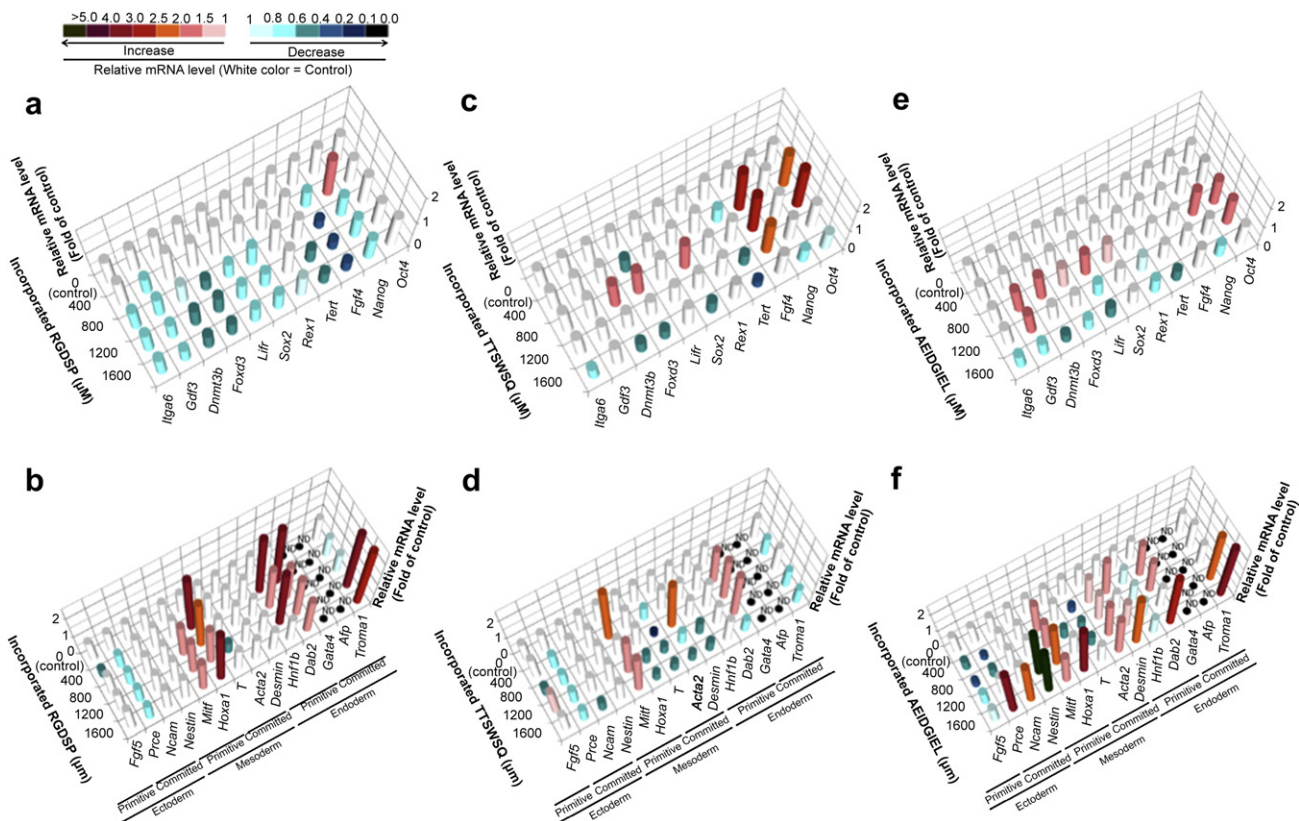

Fig. 2. Change in the expression of stemness-related (a, c and e) and differentiation-specific (b, d and f) genes in ESCs after culture in 3D scaffolds containing ECM analog peptides of different concentrations (0, 400, 800, 1200 and 1600 μM). Synthetic adhesion peptides RGDSP, a ligand for integrin $\alpha_5\beta_1$ and $\alpha_v\beta_5$ (a and b), TTSWSQ, a ligand for integrin $\alpha_6\beta_1$ (c and d) or AEIDGIEL, a ligand for integrin $\alpha_9\beta_1$ (e and f) were bound the PEG-based scaffold, and ESCs were subsequently encapsulated within the material. Gene expression was quantitatively monitored by real-time PCR at 5 d culture in the presence of LIF. In general, the expression of stemness-related gene expression was either fully maintained or significantly increased by the addition of 400, 800 and 800 μM in RGDSP, TTSWSQ and AEIDGIEL, respectively. The sequences of the peptides used in this experiment are shown in Supplementary Table 3. All data shown are means of 4 independent experiments. Different colors indicate significant difference ($p < 0.05$).

renewal, or alternatively would lead to differentiation. Zero, 400, 800, 1200 and 1600 μM of each adhesion peptide were bound individually within the scaffold. Co-activation of integrin $\alpha_5\beta_1$ and $\alpha_v\beta_5$ by 400 μM RGDSP-containing adhesion peptide led to up-regulation of only *Nanog* among the stemness-related genes examined (Fig. 2a), while *Fgf4* and *Gdf4* were down-regulated. At higher concentrations, all stemness-related genes examined were down-regulated, with the exception of *Oct4*, which was neither up- nor down-regulated at any RGDSP concentration explored. Next, integrin $\alpha_6\beta_1$ and integrin $\alpha_9\beta_1$ were activated by TTSWSQ- and AEIDGIEL-containing hydrogels (Fig. 2c,e), respectively. Activation by 800 μM TTSWSQ or AEIDGIEL strongly up-regulated the expression of most stemness-related genes (*Oct4*, *Fgf4*, *Sox2*, *Foxd3* and *Dnmt3b* by integrin $\alpha_6\beta_1$ and *Oct4*, *Nanog*, *Sox2*, *Lifr*, *Foxd3*, *Dnmt3b* and *Gdf3* by integrin $\alpha_9\beta_1$), while the same peptides of different concentrations were not suitable for the observed up-regulation. No difference in transcription was detected in *Gdf3*, *Lifr* and *Rex1* by TTSWSQ-stimulated integrin $\alpha_6\beta_1$, and *Fgf4* by AEIDGIEL-stimulated integrin $\alpha_9\beta_1$. On the other hand, extensive alterations were observed in the transcriptional levels of the differentiation-specific genes, while no dose-response behavior for up- or down-regulation was detected after the stimulations, other than a dramatic increase derived from the highest dose of AEIDGIEL (Fig. 2b,d,f). These results indicated that functional activation of several integrin heterodimers by adhesion peptide sequences being conjugated with PEG-hydrogel scaffold was critical for self-renewal of ESCs and that ligation of one integrin heterodimer alone could not trigger sufficient signal for self-renewal of ESCs.

3.5. Development of synthetic 3D integrin-stimulating matrices supporting maintenance of ESC pluripotency

To maximize the signal of integrin heterodimers for stem cell self-renewal, combinatorial conjugation of each adhesion peptide within the scaffold was conducted. Combinatorial activation of each integrin heterodimer significantly up-regulated transcription of stemness-related genes (Fig. 3a) and down-regulated transcription of differentiation-specific genes (Fig. 3b). The ESCs exposed to all three adhesion peptides for co-stimulation of $\alpha_5\beta_1$, $\alpha_v\beta_5$, $\alpha_6\beta_1$ and $\alpha_9\beta_1$ increased the transcription of all stemness-related genes, which became similar to that of ESCs cultured on MEF feeder layers. In contrast, ESCs treated with blocking antibodies of integrin heterodimers on feeder layers prominently down-regulated transcription of most stemness-related genes, which was influenced by combinatorial treatment of antibodies. Co-treatment of all antibodies for the inhibition of all integrin heterodimers induced significantly reduced transcription of all the stemness-related genes, except for *Tert*. Thus, activation of ESCs by binding to the artificial ECM via $\alpha_5\beta_1$, $\alpha_v\beta_5$, $\alpha_6\beta_1$ and $\alpha_9\beta_1$ all together maintained ESC stemness as on MEF feeder layers, and these integrins were demonstrated to be of relevance on the feeder layers as well, shown through inhibition with blocking antibodies (Supplementary Fig. 5).

On the other hand, no significant up-regulation was detected in the genes related to differentiation except for mesoderm-specific *Acta2*. Compared with the ESCs cultured on a MEF feeder layer, ectoderm- and mesoderm-specific genes were down-regulated, while no significant difference was detected in endoderm-specific genes. The translation of SSEA-1 (Fig. 4a), Oct4 (Fig. 4b), and Nanog (Fig. 4c) was maintained in the ESCs cultured within the PEG-hydrogel containing the RGDSP, TTSWSQ and AEIDGIEL peptides for 3 wk without subpassage. Especially, Nanog translation by hydrogel-embedded ESCs activated by integrin $\alpha_9\beta_1$ or all four integrin heterodimers prominently increased, which become similar to that of the ESCs cultured on the feeder layers. In addition, the ESCs cultured within the PEG-hydrogel conjugated with all three adhesion peptides formed spherical colonies (Supplementary Fig. 6) and significantly promoted proliferation and survival (Supplementary Fig. 7). However, this level of survival (mean $\pm$ S.D.; $76.3 \pm 1.33\%$) was significantly lower than those of ESCs cultured in a 2D microenvironment with ($84.5 \pm 6.95\%$) or without ($84.4 \pm 6.95\%$) a MEF feeder layer. Thus, these studies showed that a synthetic 3D microenvironment activating integrin $\alpha_5\beta_1$ and $\alpha_v\beta_5$, integrin $\alpha_9\beta_1$
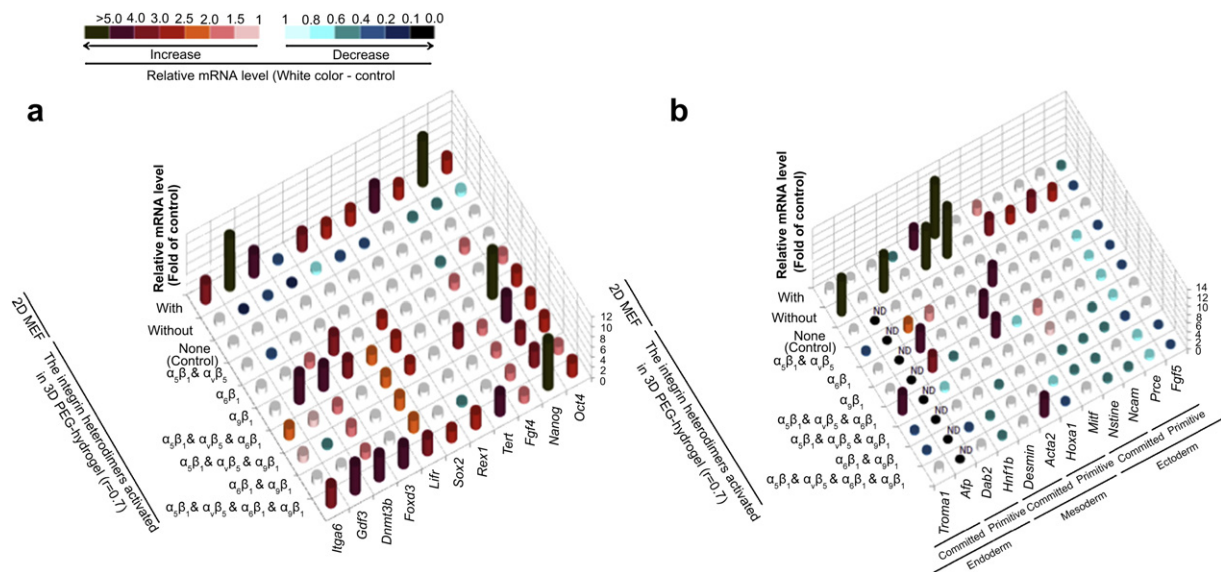

Fig. 3. Effects of combined stimulation with RGDSP ($\alpha_5\beta_1$ and $\alpha_v\beta_5$), TTSWSQ ($\alpha_6\beta_1$) and/or AEIDGIEL ($\alpha_9\beta_1$) on the expression of stemness-related (a) and differentiation-specific (b) genes in ESCs after culture in either 2D or in the 3D scaffolds. In the case of 2D culture, the ESCs were cultured in the presence (shown as with) or absence (shown as without) of a MEF feeder layer. For the construction of the 3D microenvironment, the ESCs were encapsulated into the PEG-based scaffold ($r = 0.7$) conjugated with 400 μM RGDSP, 800 μM TTSWSQ, and/or 800 μM AEIDGIEL. Gene expression of the ESCs was quantitatively monitored by real-time PCR at 5 d culture in the presence of LIF. Combined use of RGDSP, TTSWSQ and AEIDGIEL in 3D culture yielded the optimal maintenance of the ESCs, with increased expression of stemness-related genes accompanied with reduced expression of differentiation-related genes. Those levels were either comparable or superior to those observed on the 2D culture environment. All data shown are means of five independent experiments. Different colors indicate significant difference ($p < 0.05$). ND = not detected.
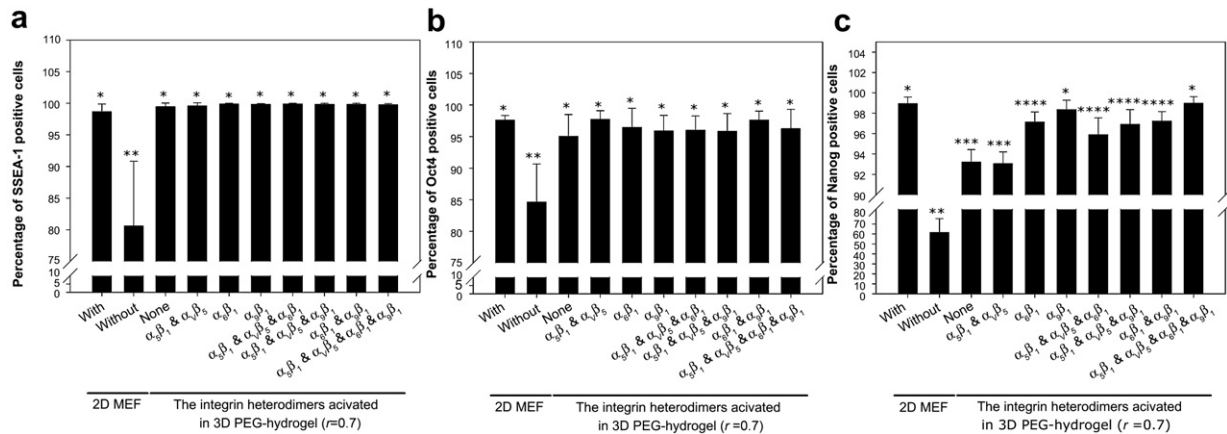
Fig. 4. Maintenance of stemness-related protein expression in ESCs cultured in either 2D or in 3D PEG-based scaffolds containing various integrin-related peptides at optimal concentrations. Maintenance of ESCs in the undifferentiated state in the 2D microenvironment was attained by the use of mitomycin C-treated MEF feeder cells, while the 3D microenvironment was created by the PEG-based scaffold ($r = 0.7$) conjugated with 400 μM RGDSP, 800 μM TTSWSQ and/or 800 μM AEIDGIEL. The ESCs were subsequently cultured for 3 wk on 2D (with subpassage every 3d) or inside the 3D microenvironment (without subpassage) in the presence of LIF, and at the end of culture, the expression of SSEA-1 (a), Oct4 (b) and Nanog (c), stem cell-specific marker proteins were evaluated by flow cytometric analysis. In all treatments for 3D culture, significant decreases in the reactivity to SSEA-1 and Oct4 were not detected after culture. Nanog expression was significantly increased in the ESCs encapsulated within the scaffold containing AEIDGIEL or all three peptides together, within which expression became similar compared with that detected in the ESCs cultured on MEF feeder cells. Dilution rate of antibodies used for flow cytometric analysis are listed in Supplementary Table 2 and all data shown are means ± S.D. of three independent experiments. *,**,***,****$p < 0.05$.

and integrin $\alpha_6\beta_1$ could effectively support self-renewal of ESCs even without feeder cells, up-regulating stemness and down-regulating differentiation-related genes.

3.6. Regulation of stemness-related signal molecule activity by downstream signaling of integrin heterodimers within 3D, RGDSP, TTSWSQ, AIEDGIEL-containing scaffolds

For identifying signal proteins regulated by downstream signaling derived from combinatorial activation of each integrin heterodimer, we investigated transcription and translation of Stat3 [34,35], β-catenin [36,37], Smad 1/5/8 [38] and Akt1 [39,40] genes and proteins, which have been reported as key signal molecules supporting stem cell self-renewal. In the case of Stat3 activated by LIF (Supplementary Fig. 8a,b,c), co-stimulation of all four integrin heterodimers stimulated *Stat3* transcription, while the stimulation of integrin heterodimers within the 3D scaffold significantly down-regulated the activation of Stat3, regardless of type of adhesion peptides. In the case of β-catenin transcription factor regulated by Wnt (Supplementary Fig. 8d,e), the highest β-catenin gene and protein expression were observed in the ESCs cultured on MEF feeder layers. There were significant transcriptional up- or down-regulations in the ESCs stimulated by specific integrin heterodimers inside a 3D scaffold. However, no translational regulation was detected and merely the absence of MEF feeder cells or the 3D scaffold prominently down-regulated β-catenin translation. In the case of Smad 1/5/8 signaling derived from BMP4 (Supplementary Fig. 9), ESCs significantly changed the transcription of *Smad 1, 5* and *8* in response to external stimulation of the integrin heterodimers. However, no alteration in the activation of Smad 1/5/8 was detected by any of these stimulations. A significant increase in the transcription of the kinase Akt1, which is activated by unknown factor-stimulated phosphoinositide 3-kinase (PI3K), was detected after the stimulation of integrin $\alpha_6\beta_1$ or all integrin heterodimers inside PEG-hydrogel (Fig. 5). Even the 3D scaffold itself, without conjugation of adhesion peptide, significantly stimulated *Akt1* transcription. However, there was no correlation between the regulation of *Akt1* transcription and that of total Akt1 translation. Mere activation of integrin $\alpha_6\beta_1$, integrin $\alpha_6\beta_1$ and $\alpha_9\beta_1$ together, or $\alpha_5\beta_1$, $\alpha_v\beta_5$, $\alpha_6\beta_1$ and $\alpha_9\beta_1$ heterodimer

signaling all together within the PEG-hydrogel significantly increased Akt1 activation. The differences in response of the ESCs between culture on MEFs and culture in the 3D matrix in terms of Smad 1/5/8, Stat3 and β-catenin activation indicate that different pathways of signal transduction can lead to the same overall cellular phenotype of maintenance of the undifferentiated state. Still, based on the results, we can presume that this Akt1 signal has a critical effect on stem cell self-renewal and survival within this material.

4. Discussion

Numerous signals must be integrated by the ESCs within the niche, to drive self-renewal versus differentiation decisions. Many of these derived from the ECM, however the roles they play, in alternately supporting self-renewal or differentiation, remains unclear. To address this, we developed an artificial ECM analog, with which we could explore the role of integrin ligation and activation on ESC fate decisions. Through transcriptional analysis of 24 integrin subunits, followed by confirmation at the protein level and inhibition with blocking antibodies, we identified $\alpha_5\beta_1$, $\alpha_v\beta_5$, $\alpha_6\beta_1$ and $\alpha_9\beta_1$ as interesting. Using the 3D hydrogel microenvironment as an experimental tool, we determined that activation of these four integrins together, but not alone, led to up-regulation of stemness genes and down-regulation of differentiation genes. Integrin signaling apparently plays a role in ESC interaction with feeder cells as well, in that blocking binding of these same integrins on MEF feeder layers also inhibited maintenance of stemness. Within the hydrogel that binds $\alpha_5\beta_1$, $\alpha_v\beta_5$, $\alpha_6\beta_1$ and $\alpha_9\beta_1$, Akt1-derived signal transduction along with regulation of other stemness-related gene appears to be a major key for maintaining self-renewal of ESCs and inducing additional morphogenesis such as the formation of spherical colonies.

From a practical perspective, the hydrogels presented herein may be useful not just to study the roles of integrins in ESC decision making, but also as a substrate for ESC self-renewal in culture, in the absence of MEF feeder cells. We note that other approaches, both based on matrices [5,41] and molecular [36,38] approaches have been presented. The matrix approach described here is particularly flexible, and moreover may be useful in investigating
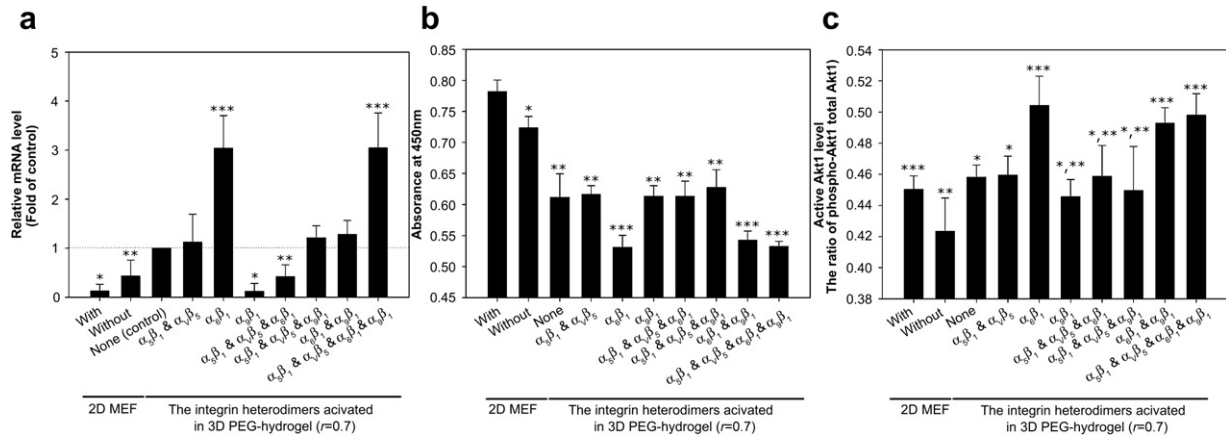
Fig. 5. Transcription and translation of Akt1 signal protein resulted from dimensional differences and combinatorial activation of integrin heterodimers by peptide sequences in ESCs. Maintenance of the undifferentiated ESCs in the 2D microenvironment was obtained use of mitomycin C-treated MEFs, while the 3D microenvironment was created by PEG-based scaffolds ($r = 0.7$). Combinatorial activation of integrin heterodimers in ESCs encapsulated within the PEG-based scaffold was achieved by conjugation of 400 μM RGDSP ($\alpha_5\beta_1$ and $\alpha_v\beta_5$), 800 μM TTSWSQ ($\alpha_6\beta_1$) and/or 800 μM AEIDGIEL ($\alpha_9\beta_1$) to PEG-VS. On d5 of culture in 2D (with subpassage every 3 d) or within the 3D microenvironment (without subpassage) in the presence of LIF, expression of *Akt1* (a) was quantified by real-time PCR. In 3D culture, the combinatorial stimulation of all integrin heterodimers together induced significant increase in gene transcription of *Akt1*, and the 3D scaffold itself greatly increased *Akt1* gene expression. In a 2D microenvironment, MEF feeders down-regulated *Akt1* gene expression. All data derived from real-time PCR indicate means ± S.D. of four independent experiments. Subsequently, the expression of stemness-related signal proteins of Akt1 (b) and phospho-Akt1 (c) were analyzed by ELISA, and the active level of Akt1 signal proteins were represented as the ratio of absorbance of phospho-proteins to absorbance of total proteins. Integrin $\alpha_6\beta_1$, co-stimulation of integrin $\alpha_6\beta_1$ and $\alpha_9\beta_1$, and stimulation of all the integrin heterodimers together strongly stimulated Akt1 activation, while total Akt1 translation was lowered. The 3D scaffold itself significantly increased the active level of Akt1 protein and concomitantly inhibited total Akt1 protein translation. All data derived from ELISA indicate means ± S.D. of five independent experiments. *,**,***$p < 0.05$.

and applying the influence of matrix interactions in the niche upon stem cell self-renewal and differentiation more generally.

5. Conclusions

We present an approach by which to qualitatively and quantitatively characterize the requirements for integrin ligation in the embryonic stem cell microenvironment necessary for maintenance of stemness. The hydrogel material allows systematic modulation of mechanics, adhesion ligand(s), amounts of adhesion ligands, and proteolytic sensitivity. Although we have demonstrated the approach here with embryonic stem cells, the method is equally applicable to adult stem cells as well. From the perspective of the analysis we performed on murine embryonic stem cells, we applied the method to demonstrate a critical role of simultaneous signaling from identified $\alpha_5\beta_1$, $\alpha_v\beta_5$, $\alpha_6\beta_1$ and $\alpha_9\beta_1$ in maintenance of stemness. This combination of integrins may specific to murine embryonic stem cells, and comparative analysis in human embryonic stem cells is both necessary and under way.

Acknowledgements

Appendix. Supplementary data

Supplementary data associated with this article can be found in the online version, at doi:10.1016/j.biomaterials.2009.10.054.

References

[1] Mallon BS, Park K-Y, Chen KG, Hamilton RS, McKay RDG. Toward xeno-free culture of human embryonic stem cells. Int J Biochem Cell Biol 2006;38:1063–75.

[2] Skottman H, Hovatta O. Culture conditions for human embryonic stem cells. Reproduction 2006;132:691–8.

[3] McDevitt TC, Palecek SP. Innovation in the culture and derivation of pluripotent human stem cells. Curr Opin Biotechnol 2008;19:527–33.

[4] Li YJ, Chung EH, Rodriguez RT, Firpo MT, Kevin E. Healy. Hydrogels as artificial matrices for human embryonic stem cell self-renewal. J Biomed Mater Res A 2006;79:1–5.

[5] Nur-E-Kamal A, Ahmed I, Kamal J, Schindler M, Meiners S. Three-dimensional nanofibrillar surfaces promote self-renewal in mouse embryonic stem cells. Stem Cells 2006;24:426–33.

[6] Kloxin AM, Kasko AM, Salinas CN, Anseth KS. Photodegradable hydrogels for dynamic tuning of physical and chemical properties. Science 2009;324:59–63.

[7] Hynes RO. Integrins: bidirectional, allosteric signaling machines. Cell 2002;110:673–87.

[8] Hata RI. Where am I? How a cell recognizes its positional information druing morphogenesis. Cell Biol Int 1996;20:59–65.

[9] Boudreau N, Bissell MJ. Extracellular matrix signaling: integration of form and function in normal and malignant cells. Curr Opin Cell Biol 1998;10:640–6.

[10] Danen EH, Yamada KM. Fibronectin, integrins, and growth control. J Cell Physiol 2001;189:1–13.

[11] Ramirez F, Rifkin DB. Cell signaling events: a view from the matrix. Matrix Biol 2003;22:101–7.

[12] Cooper AR, MacQueen HA. Subunits of laminin are differentially synthesized in mouse eggs and early embryos. Dev Biol 1983;96:467–71.

[13] George EL, Georges-Labouesse EN, Patel-King RS, Rayburn H, Hynes RO. Defects in mesoderm, neural tube and vascular development in mouse embryos lacking fibronectin. Development 1993;119:1079–91.

[14] Fässler R, Meyer M. Consequences of lack of beta 1 integrin gene expression in mice. Genes Dev 1995;9:1896–908.

[15] Stephens LE, Sutherland AE, Klimanskaya IV, Andrieux A, Meneses J, Pedersen RA, et al. Deletion of beta 1 integrins in mice results in inner cell mass failure and peri-implantation lethality. Genes Dev 1995;9:1883–95.

[16] Li S, Harrison D, Carbonetto S, Fassler R, Smyth N, Edgar D, et al. Matrix assembly, regulation, and survival functions of laminin and its receptors in embryonic stem cell differentiation. J Cell Biol 2002;157:1279–90.

[17] Watt FM, Hogan BL. Out of eden: stem cells and their niches. Science 2000;287:1427–30.

[18] Czyz J, Wobus A. Embryonic stem cell differentiation: the role of extracellular factors. Differentiation 2001;68:167–74.

[19] Williams DA, Rios M, Stephens C, Patel VP. Fibronectin and VLA-4 in haematopoietic stem cell-microenvironment interactions. Nature 1991;352:438–41.

[20] Zhu AJ, Haase I, Watt FM. Signaling via beta1 integrins and mitogen-activated protein kinase determines human epidermal stem cell fate in vitro. Proc Nat Acad Sci USA 1999;96:6728–33.

[21] Campos LS, Leone DP, Relvas JB, Brakebusch C, Fassler R, Suter U, ffrench-Constant C. Beta1 integrins activate a MAPK signalling pathway in neural stem cells that contributes to their maintenance. Development 2004;131:3433–44.

[22] Lutolf MP, Hubbell JA. Synthetic biomaterials as instructive extracellular microenvironments for morphogenesis in tissue engineering. Nat Biotechnol 2005;23:47–55.

[23] Lutolf MP, Weber FE, Schmoekel HG, Schense JC, Kohler T, Muller R, et al. Repair of bone defects using synthetic mimetics of collagenous extracellular matrices. Nat Biotechnol 2003;21:513–8.

[24] Lutolf MP, Tirelli N, Cerritelli S, Cavalli L, Hubbell JA. Systematic modulation of Michael-type reactivity of thiols through the use of charged amino acids. Bioconj Chem 2001;12:1051–6.

[25] Lutolf MP, Hubbell JA. Synthesis and physicochemical characterization of end-linked poly(ethylene glycol)-co-peptide hydrogels formed by Michael-type addition. Biomacromolecules 2003;4:713–22.

[26] Cooper HM, Tamura RN, Quaranta V. The major laminin receptor of mouse embryonic stem cells is a novel isoform of the alpha 6 beta 1 integrin. J Cell Biol 1991;115:843–50.

[27] Fassler R, Pfaff M, Murphy J, Noegel A, Johansson S, Timpl R, et al. Lack of beta 1 integrin gene in embryonic stem cells affects morphology, adhesion, and migration but not integration into the inner cell mass of blastocysts. J Cell Biol 1995;128:979–88.

[28] Raeber GP, Lutolf MP, Hubbell JA. Molecularly engineered PEG hydrogels: a novel model system for proteolytically mediated cell migration. Biophys J 2005;89:1374–88.

[29] Pierschbacher MD, Ruoslahti E. Cell attachment activity of fibronectin can be duplicated by small synthetic fragments of the molecule. Nature 1984;309:30–3.

[30] Mardilovich A, Kokkoli E. Biomimetic peptide-amphiphiles for functional biomaterials: the role of GRGDSP and PHSRN. Biomacromolecules 2004;5:950–7.

[31] Maubant S, Saint-Dizier D, Boutillon M, Perron-Sierra F, Casara PJ, Hickman JA, et al. Blockade of $\alpha v \beta 3$ and $\alpha v \beta 5$ integrins by RGD mimetics induces anoikis and not integrin-mediated death in human endothelial cells. Blood 2006;108:3035–44.

[32] Leu SJ, Liu Y, Chen N, Chen C-C, Lam SC-T, Lau LF. Identification of a novel integrin $\alpha 6 \beta 1$ binding site in the angiogenic inducer CCN1 (CYR61). J Biol Chem 2003;278:33801–8.

[33] Yokosaki Y, Matsuura N, Higashiyama S, Murakami I, Obara M, Yamakido M, et al. Identification of the ligand binding site for the integrin alpha 9 beta 1 in the third fibronectin type III repeat of tenascin-C. J Biol Chem 1998;273:11423–8.

[34] Niwa H, Burdon T, Chambers I, Smith A. Self-renewal of pluripotent embryonic stem cells is mediated via activation of STAT3. Genes Dev 1998;12:2048–60.

[35] Matsuda T, Nakamura T, Nakao K, Arai T, Katsuki M, Heike T, et al. STAT3 activation is sufficient to maintain an undifferentiated state of mouse embryonic stem cells. EMBO J 1999;18:4261–9.

[36] Sato N, Meijer L, Skaltsounis L, Greengard P, Brivanlou AH. Maintenance of pluripotency in human and mouse embryonic stem cells through activation of Wnt signaling by a pharmacological GSK-3-specific inhibitor. Nat Med 2004;10:55–63.

[37] Miyabayashi T, Teo J-L, Yamamoto M, McMillan M, Nguyen C, Kahn M. Wnt/ β-catenin/CBP signaling maintains long-term murine embryonic stem cell pluripotency. Proc Nat Acad Sci USA 2007;104:5668–73.

[38] Ying QL, Nichols J, Chambers I, Smith A. BMP induction of Id proteins suppresses differentiation and sustains embryonic stem cell self-renewal in collaboration with STAT3. Cell 2003;115:281–92.

[39] Watanabe S, Umehara H, Murayama K, Okabe M, Kimura T, Nakano T. Activation of Akt signaling is sufficient to maintain pluripotency in mouse and primate embryonic stem cells. Oncogene 2006;25:2697–707.

[40] Hayashi Y, Furue MK, Okamoto T, Ohnuma K, Myoishi Y, Fukuhara Y, et al. Integrins regulate mouse embryonic stem cell self-renewal. Stem Cells 2007;25:3005–15.

[41] Greenlee AR, Kronenwetter-Koepel TA, Kaiser SJ, Liu K. Comparison of Matrigel™ and gelatin substrata for feeder-free culture of undifferentiated mouse embryonic stem cells for toxicity testing. Toxicol In Vitro 2005;19:389–97.